



EXPERIMENTAL LOCALIZATION OF A POLE OF THE REFLECTION
COEFFICIENT OF A POROUS LAYER

J. TIZIANEL AND J.-F. ALLARD

*Institut d'Acoustique et de Mécanique de l'Université du Maine, URA 1101 CNRS,
Avenue O. Messiaen, B.P. 535, 72017 Le Mans Cedex, France*

AND

W. LAURIKS AND L. KELDERS

*Laboratorium voor Akoestiek en Thermische Fysica, Katholieke Universiteit Leuven,
Department Natuurkunde, Celestijnenlaan 200 D, 3001 Heverlee, Belgium*

(Received 24 June 1996, and in final form 18 September 1996)

1. INTRODUCTION

Several experiments have indicated the presence of a surface wave above a comb-like structure [1, 2], but setting in evidence a surface wave above a porous layer is less simple [3]. Some information about the pole of the first kind of the reflection coefficient of a porous layer, related to a surface wave, are briefly recalled in this introduction. In the next section, experimental evidence of this pole is shown, and the main properties of the corresponding surface wave are indicated. The reflection coefficient of a porous layer set on a rigid impervious backing (see Figure 1) can be written in the context of equivalent fluid models [4] as

$$R = \frac{m \cos \theta + jn \cos \theta_1 \phi \operatorname{tg}(k_1 l \cos \theta_1)}{m \cos \theta - jn \cos \theta_1 \phi \operatorname{tg}(k_1 l \cos \theta_1)}. \quad (1)$$

In this equation, m and n are, respectively,

$$m = \rho_{ef}/\rho_0, \quad (2)$$

where ρ_0 is the density of air and ρ_{ef} is the effective density of the fluid equivalent to air in the porous medium, and

$$n = k_1/(\omega/c), \quad (3)$$

where k_1 is the wavenumber in the porous medium, c is the sound speed in free air, and ω is the radian frequency. The porosity of the porous medium is ϕ , the thickness of the layer l , and θ_1 is the angle of refraction, related to the angle of incidence θ by

$$n \sin \theta_1 = \sin \theta. \quad (4)$$

The time dependence is $\exp(-j\omega t)$ as in the book by Brekhovskikh and Godin [5]. The direction of the z -axis normal to the surface of the layer, and the main notations are also the same as in this book.

It has been shown previously that the poles of the reflection coefficient of a porous layer can be classified in two categories, the pole of the first kind and an infinite number of poles

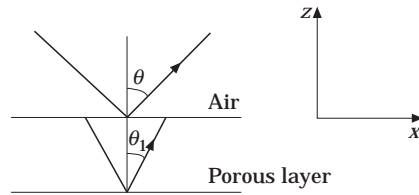


Figure 1. A porous layer reflects an incident wave under an angle of incidence θ . The angle of refraction is θ_1 .

of the second kind [4]. For $|k_1 l| \ll 1$, the pole of the first kind is, at the fourth order approximation, given by [4]

$$\sin \theta_q = 1 + \frac{\phi^2 k_1^2 l^2}{2n^2 m^2} (n^2 - 1)^2 \left[1 + \left(1 - \frac{1}{n^2} \right) k_1^2 l^2 \left(\frac{1}{3} - \frac{\phi^2}{m^2} \right) \right]^2. \quad (5)$$

The real part of $\sin \theta_q$ is close to, and larger than one, and the imaginary part small and positive. The poles of the second kind, for $|k_1 l| \ll 1$ are far from the real $\sin \theta$ axis and do not have a clear effect on the reflection coefficient measured on the real axis. As an example, the trajectory of the pole of the first kind is represented in Figure 2 in the $\sin \theta$ plane for a porous layer of thickness equal to 2.5 cm made of a fibrous material described in a previous work [6]. The parameters that characterize the material are given in the Appendix with a brief description of the modelling used to predict k_1 and ρ_{ef} . The trajectory of the pole is obtained by a method described in reference [4], and is compared with the approximated trajectory obtained with the help of equation (5). There is a good agreement for frequencies below 500 Hz between the exact and the approximated values of $\sin \theta_q$. The pole is close to the real axis at low frequencies and will have an important influence on the reflection coefficient measured on the real axis.

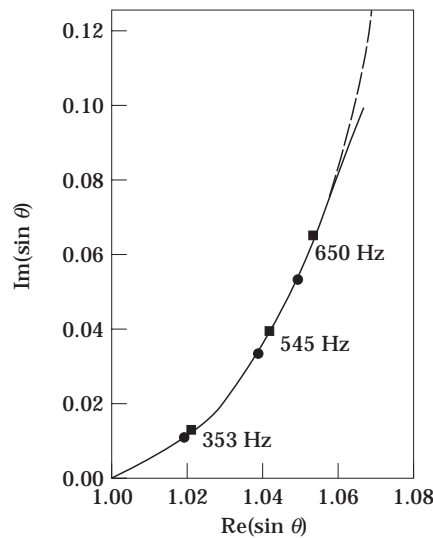


Figure 2. The trajectory of the pole of the first kind for the material described in the Appendix. —●—●—●—, Exact location; —■—■—■—, approximate location from equation (1).

2. MEASUREMENT OF THE REFLECTION COEFFICIENT AND COMPARISON WITH PREDICTIONS

The near-field acoustical holography method (NAH) developed by Tamura [7, 8] can be used to measure the reflection coefficient on the real $\sin \theta$ axis for $\sin \theta > 1$. A sound source is set above the porous layer. The method is based on the use of a two-dimensional Fourier transform to measure the amplitude of the incident and the related reflected plane wave components of the acoustics field created by the source. The method can be used for plane waves having a projection of the wavenumber vector parallel to the surface of the layer real and larger than the wavenumber in air. For such waves, which are created by a usual source, $\sin \theta_q$ is real and larger than one. The source, for the experimental set developed in Le Mans, is a loudspeaker and the acoustic field is axisymetrical around a normal to the surface of the layer. A simple mono-dimensional Hankel transform instead of the two-dimensional Fourier transform is used. The reflection coefficient, measured and predicted from equation (1), is represented in Figure 3 at 545 Hz. Fast variations appear between $\sin \theta = 1$ and 1.1. The measured and predicted behaviors of the real and the imaginary parts of R are very similar. The variations are faster at lower frequencies, because the pole is closer to the real axis. The measured and predicted values of $\sin \theta$ at which $|R|$ presents a maximum are shown in Figure 4 as functions of frequency, and compared to the predicted real part of $\sin \theta_q$. The predicted and measured locations of the maxima are surprisingly close to each other. These maxima are close to $\text{Re}(\sin \theta_q)$ only for low frequencies, when the distance between the pole and the real axis is sufficiently small. It appears that at low frequencies, $\text{Re}(\sin \theta)$ for the pole of the first kind can be evaluated from the location of the maximum of $|R|$.

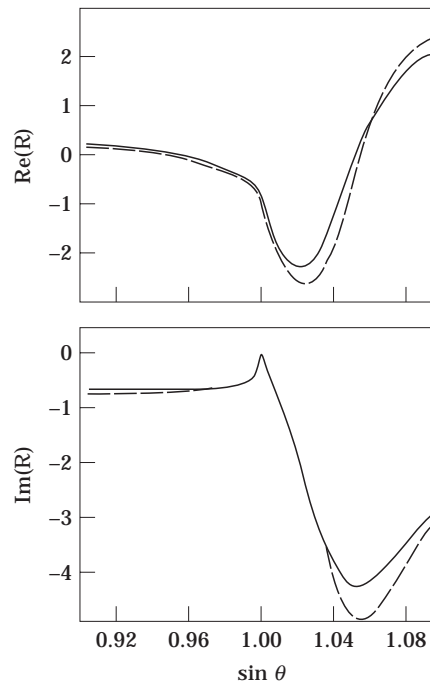


Figure 3. The reflection coefficient for $\sin \theta$ real and close to the pole for the material described in the Appendix at 545 Hz. —, Measurement; - - -, prediction.

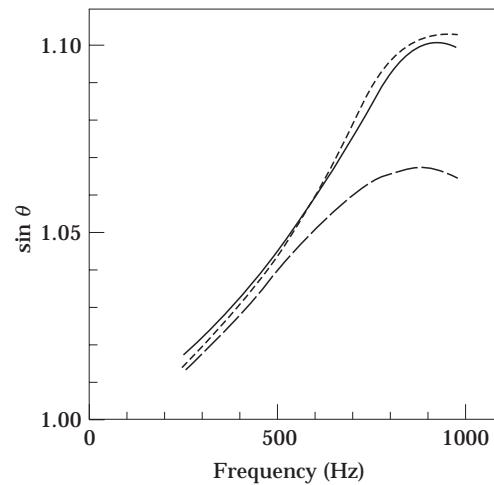


Figure 4. Location of the maximum of the reflection coefficient modulus on the $\text{Re}(\sin \theta)$ axis and $\text{Re}(\sin \theta)$ for the pole of the first kind versus frequency for the material described in the Appendix. —, Measurement; ----, prediction; — · —, $\text{Re}(\sin \theta)$ for the pole of the first kind, prediction.

3. CHARACTERIZATION OF THE SURFACE WAVE RELATED TO THE POLE

Only the real part of $\sin \theta_q$ can be evaluated, at low frequencies, from the measured location of the maximum of $|R|$, but the agreement between the predicted and measured real and imaginary parts of R suggests that equation (1) gives correct orders of magnitude for the imaginary part of $\sin \theta_q$. As an example, for the material considered, $\sin \theta_q$ and $\cos \theta_q$, obtained from equation (1), and the maximum value for $|R|$, are given in Table 1 at 250 Hz and 500 Hz.

It has been shown that the reflected wave related to the pole of the first kind at low frequencies is a true surface wave [9], but this wave is difficult to set in evidence over a porous layer. This can be explained by the orders of magnitude of $\sin \theta_q$, $\cos \theta_q$ and $\text{Max } |R|$, in Table 1. The speed of the surface wave in the x direction, obtained from the real part of $\sin \theta_q$, is very close to the speed of sound in free air at 250 Hz, and the damping in the z direction is weak. The difference in velocity and the damping increase with frequency but simultaneously the maximum of $|R|$ decreases, so that the amplitude of the surface wave created by a point source above a porous layer is much smaller than for the case of a comb-like structure.

4. CONCLUSIONS

The NAH method can be used to measure the reflection coefficient of a porous layer for waves evanescent in the direction normal to the surface of the layer. A pole of the

TABLE 1

Values of $\sin \theta_q$, $\cos \theta_q$ and $\text{Max } |R|$ for a layer of thickness equal to 2.5 cm of the material described in the Appendix

	250 Hz	500 Hz
$\sin \theta_q$	$1.0117 + j4.191 \times 10^{-3}$	$1.0391 + j3.129 \times 10^{-2}$
$\cos \theta_q$	$-2.719 \times 10^{-3} + j1.559 \times 10^{-1}$	$-1.0807 \times 10^{-1} + j3.0085 \times 10^{-1}$
$ R $	11.5	5.7

reflection coefficient, and the related surface wave, can be set in evidence with this method. The measurements are in a good agreement with a previous description of the poles. It appears that the surface wave above a porous layer is not easily detectable by simple methods which can be used for the case of a comb-like structure, due to its weak amplitude when it is noticeably different from a simple plane wave in free air.

REFERENCES

1. K. M. IVANOV-SHITS and F. V. ROZHIN 1960 *Soviet Physics Acoustics* **5**, 510. Investigation of surface wave in air.
2. G. A. DAIGLE, M. R. STINSON and D. HAVELOCK 1996 *Journal of the Acoustical Society of America* **99**, 1993–2005 Experiments on surface waves over a model impedance plane.
3. D. G. ALBERT 1992 in *Proceedings of the 5th International Symposium on Long Range Sound Propagation (Milton Keynes, U.K.)*, 10–16. Observation of acoustic surface waves propagating above a snow cover.
4. W. LAURIKS, L. KELDERS and J.-F. ALLARD 1996 *Internal Report, K. V. Leuven* Poles and zeros of the reflection coefficient of a porous layer having a motionless frame.
5. L. M. BREKHOVSKIKH and O. A. GODIN 1992 *Acoustics of Layered Media, II: Point Source and Bounded Beams* (Springer Series on Wave Phenomena). New York: Springer-Verlag.
6. B. BROUARD, D. LAFARGE and J. F. ALLARD 1994 *Acta Acustica* **2**, 301 Measurement and prediction of the surface impedance of a resonant sound absorbing structure.
7. M. TAMURA 1990 *Journal of the Acoustical Society of America* **88**, 2259–2264 Spatial Fourier transform method of measuring reflection coefficient of porous layers at oblique incidence.
8. B. BROUARD, D. LAFARGE, J.-F. ALLARD and M. TAMURA 1996 *Journal of the Acoustical Society of America* **99**, 100–107 Measurement and prediction of the reflection coefficient of porous layers at oblique incidence and for inhomogeneous waves.
9. J. NICOLAS and J.-F. ALLARD *Submitted to Journal of the Acoustical Society of America* Surface waves above a porous layer and Tolstoy criterion.
10. Y. CHAMPOUX and J.-F. ALLARD 1991 *Journal of Applied Physics* **70**, 1975–1979 Dynamic tortuosity and bulk modulus in air-saturated porous media.
11. D. L. JOHNSON, J. KOPLIK and R. DASHEN 1987 *Journal of Fluid Mechanics* **176**, 379–402 Theory of dynamic permeability and tortuosity in fluid saturated porous media.

APPENDIX: THE POROUS MATERIAL AND THE EQUIVALENT FLUID

Air in the porous material can be replaced by a fluid that occupies a volume ϕ per unit volume of porous material. The bulk modulus χ_1 of this fluid is calculated by taking into account the thermal exchange between the air inside the layer and the frame. The concept of thermal length [10] is used, and the thermal exchanges are modelled in a first approximation as in circular cylinders of radius equal to the thermal length A' . The effective density of the fluid is predicted by using the model worked out by Johnson *et al.* [11]. The wavenumber k_1 inside the layer is given by

$$k_1 = \omega(\rho_{ef}/\chi_1)^{1/2}. \quad (\text{A1})$$

The parameters which characterize the porous material were determined in a previous study. They are given in Table A1.

TABLE A1

The parameters that characterize the porous material; the thickness of the layer is equal to 2.5 cm

Flow resistivity, σ (Nm ⁻⁴ s)	Tortuosity, α_∞	Porosity, ϕ	Viscous length, A (m)	Thermal length, A' (m)
33 000	1.1	0.98	0.5×10^{-4}	1×10^{-4}